Computational and Theoretical Chemistry 993 (2012) 7–12

Contents lists available at SciVerse ScienceDirect

Computational and Theoretical Chemistry

journal homepage: www.elsevier.com/locate/comptc

Bipolarons and polaron pairs in oligopyrrole dications

Yafei Dai [a,b], Chengwei Wei [a], Estela Blaisten-Barojas [b,c,*]

[a] School of Physics Science and Technology, Nanjing Normal University, Nanjing 210097, People's Republic of China
[b] Computational Materials Science Center, George Mason University, Fairfax, VA 22030, USA
[c] School of Physics, Astronomy, & Computational Sciences, George Mason University, Fairfax, VA 22030, USA

ARTICLE INFO

Article history:
Received 22 March 2012
Received in revised form 11 May 2012
Accepted 11 May 2012
Available online 30 May 2012

Keywords:
Oligopyrrole
Polaron pairs
Bipolaron
Density functional theory

ABSTRACT

A series of oligopyrrole dications, n-Py^{2+}, n = 1–12, 15, 18, 21, 24, 27 are studied with hybrid density functional theory at the B3PW91/6-31+G(d,p) level. Geometry optimization and electronic structure of oligopyrrole dications are revisited using spin-restricted and spin-unrestricted methods. It is found that the ground states of short oligopyrrole dications n-Py^{2+} ($n < 7$) are spin-restricted singlet ground states. Thus, the charge carrier in these molecular dications has characteristics of a bipolaron. In contrast, medium size oligopyrrole dications ($7 \leqslant n \leqslant 15$) have a spin-unrestricted singlet ground state and display charge carriers that have a polaron pair character. With increasing oligomer length, the spin-unrestricted singlet and the triplet become degenerate such that for even longer oligopyrrole dications (n-Py$^{2+}, n \geqslant 18$) the ground state is a triplet and the charge carrier is predominantly a polaron pair.

1. Introduction

A major challenge in the study of conducting polymers is to understand the mechanism of charge transport. A fundamental question in understanding the conductivity of oxidized polypyrroles (PPys) is the characterization of the charge carriers. Indeed, carriers may be spinless bipolarons [1–3] or spin-carrying polarons [1,2,4]. The design of new materials with improved properties such as light emitting diodes (LEDs) [5], photovoltaic cells [6] and artificial muscles [7] would benefit if the dichotomy is resolved. Polythiophene has been the most studied conducting polymer. However, even for this polymer, contradictory opinions exist concerning the conducting mechanism. Semiempirical calculations predicted that two polarons on the oligothiophene chain would be more stable than one bipolaron for oligomers longer than the dodecamer [8]. Brocks [9], using local density functional theory, proposed that the polaron pair was a stable charge carrier in oligothiophenes while bipolaron formation was unstable with respect to separation into polarons. Contrarily, Silva's theoretical study [10] showed that the bipolaron structure is dominant for highly doped polythiophene. Recent hybrid density functional studies of oligothiophenes [11,12] stated that the bipolaron formation was predominant over polaron pairs for short oligothiophene dications while both bipolaron and polaron pair contributed to the carrier structure for medium size oligothiophene dications. These authors reported that the polaron pair became dominant for long oligothiophene dications. Various experiments also reported contradictory assignments for distinguishing between bipolaron and polaron pairs [13–17].

Polypyrrole (PPy) is another prototypical conducting polymer for which much less has been discovered concerning the mechanism of conduction. In fact, the mechanism of conduction in PPy is still open for discussion. According to Heeger et al. [18], the formation of bipolaron species in conjugated polymers is energetically favorable as compared to the formation of two polarons. Bredas and Street [19] combined UV–vis measurements of PPy at different oxidation levels with theoretical calculations to correlate the evolution of the UV–vis absorption bands with the formation of polaron and bipolaron species. They asserted that the spinless bipolaron was the charge carrier of preference. Shimoi et al. [20] using density-matrix renormalization group studied the stability of polaron and bipolaron in conjugated polymers and found that the charge distribution changed from polaron to bipolaron with increasing doping level. In situ Raman spectro-electrochemistry has been used to study polaron and bipolaron formation in PPy by Santos et al. [21]. These authors showed that as PPy was oxidized from the neutral pristine state, a transient new phase featuring both benzenoid and quinoid phases was observed. They correlated this intermediary phase with polaron formation. Theoretical studies of PPy and oligopyrroles n-Py, n = 2–24 (n being the number of monomer rings) have mainly been restricted to the structural, energetic and electronic properties with emphasis in high doping concentration [22–27]. A thorough understanding of the nature of charge carriers in oligopyrrole chains merits further study.

* Corresponding author. Address: Computational Materials Science Center, George Mason University, 4400 University Dr, MS 6A2, Fairfax, VA 22030, USA. Fax: +1 703 993 9300.
E-mail address: blaisten@gmu.edu (E. Blaisten-Barojas).

2210-271X/$ - see front matter © 2012 Elsevier B.V. All rights reserved.
http://dx.doi.org/10.1016/j.comptc.2012.05.018

In this work we present a density functional theory study of oligopyrrole dications with emphasis on the spin behavior of the molecular wave function associated with types of charge localization characterizing oligomers of different lengths. The spin-restricted and spin-unrestricted singlet ground states of n-Py^{2+} ($n = 2$—24) are investigated with the goal of clarifying whether polaron pairs or bipolaron structures are predominant in the oligopyrrole dications. This paper is organized as follows. Section 2 describes the methodology used. Section 3 describes the geometrical configurations and electronic properties of n-Py dications as well as the discussion for the formation of the polaron pairs and bipolarons. This paper is concluded in Section 4.

2. Theoretical methods

Density functional theory (DFT) and the hybrid Becke–Perdew–Wang 1991 (B3PW91) approach [28–30] are used throughout this study, which includes local and nonlocal correlation functionals. A double valence basis set 6-31+G(d,p) with diffuse and polarization functions for all atoms is adopted in all calculations [31]. Larger basis sets 6-311+G(d,p) were used for 18-Py, which showed comparable results with the 6-31+G(d,p). Therefore, in this paper we report calculations based on the latter only. The Gaussian 03 package [32] is used throughout. The choice of the correlation functional is based on comparative results of Py structure using a variety of functionals: B3PW91 [29,30], B3LYP [33,34], B3BMK [35], PBE [36] and M06-HF [37]. Results closest to experiment [38,26] are obtained with B3PW91, reproducing the experimental planar structure of pyrrole (Py) with the smallest error of 1.0%. The B3PW91 approach is then adopted, which additionally allows for comparison with our previous studies [23–25]. The Py molecule is a C_{2v} planar structure with a strong dipole moment of 1.94D in the direction of the N—H bond and -23.5, -26.8, $-34.4D$ Å for the diagonal elements of the quadrupole matrix.

Geometry optimization for each n-Py oligomer ($n = 1$—$12, 15, 18, 21, 24, 27$) and its corresponding oligomer dication were attained by minimizing the molecular electronic energy with respect to coordinates of all atoms in 3D using the Berny algorithm and redundant internal coordinates [39,40]. Optimizations ensured accuracies of 10^{-4} Bohr for distances and 10^{-8} Hartrees for energies. The geometry conformations of n-Py and n-Py^{2+} were optimized with anti-gauche arrangements of the monomers [23]. The frequency analysis was performed for stable singlet and triplet states of neutral and dication oligomers with lengths up to 12-Py. A frequency analysis of these geometry optimized structures yielded positive frequencies, indicating that such structures corresponded to minima of the electronic energy. For oligomers longer than 12-Py, the vibrational frequency calculation was beyond our present computational ability. Mulliken population analysis and the natural population analysis (NPA) are used to calculate the atomic charges of the oligopyrrole dications. Electronic states of the oligopyrrole dications are calculated in spin-restricted (RB3PW91) and spin-unrestricted (UB3PW91) singlet states and in the triplet state.

3. Bipolaron versus polaron pair in oxidized nPy^{2+} oligomers

Spin-restricted and spin-unrestricted hybrid DFT have been used in the past for investigating the transition from bipolaron to two-polarons in doubly charged oligothiophenes [11,41]. In this work we follow the approach of these authors to investigate the localization of positive charge (hole) in dication oligopyrrole chains. A spin-restricted singlet calculation, RB3PW91, corresponds to formation of a bipolaron (one spatially localized hole of +2e) and zero spin for the system while the unrestricted calculations, UB3PW91, signals the appearance of a polaron pair (two spatially localized holes, each of +e) with system spin either zero or one. We find that the spin-restricted approach for short oligomer dications up to 6-Py^{2+} yields a stable spin-restricted singlet ground state. Indeed, the square of the spin S^2 of n-Py^{2+} ($n = 5, 6$) is zero. Thus, dications of short oligopyrroles exhibit spinless bipolaron formation. However, dications of longer oligopyrroles n-Py^{2+} ($n > 6$) exhibit a significant contribution of polaron pair character in their ground state (two spatially separated cation radicals within the same molecule). This is evidenced by the appearance of an instability in the RB3PW91 solution of the singlet state while the spin-unrestricted solution is stable, highlighting the diradical character of the wavefunction in oligopyrrole dications with lengths up to 15-Py^{2+}. Indeed, these medium-sized oligomer dications n-Py^{2+} ($6 < n < 16$) posses a triplet state located very close in energy above the singlet ground state and the ground state wave function acquires a mixed singlet–triplet character. Additionally, S^2 is not zero after annihilation. As a consequence, medium-sized oligomer dications display a splitting of one bipolaron into two polarons. This pair of polarons are associated with two intramolecular cation radicals with opposite spin such that the state is a singlet. For 18-Py^{2+} and longer oligopyrrole dications the triplet state becomes their ground state. Oligomer dications with long chains have polaron pair configuration arising from the triplet state character of the wave function. These observations indicate that the polaron pair character of the ground-state is increasingly important as the oligomer length increases. Table 1 gives the binding energies (total energy referred to the energy of the separated neutral atoms divided by n, the number of monomers in the oligomer) of the oligomer dications in the singlet and triplet states.

In addition, following Ref. [42], an estimate of the singlet ground state energy eliminating the singlet–triplet mixing can be calculated from $E_{singlet} = (E - aE_{s+1})/(1 - a)$, with $a = (< S^2 > - s(s+1))/2(s+1)$. Estimated energies of the singlet state are reported in the fourth column of Table 1, showing that the singlet estimate is lower in energy than the calculated singlet state for chains up to 15-Py^{2+}. For longer chains the estimated singlet displays a slight energy destabilization, evidencing that the ground state is the triplet state.

The top of Fig. 1 shows the numbering scheme given to bonds in a portion of neutral PPy. In Fig. 1a–d, the black line depicts C—C bond lengths in the conjugated π chain of the neutral oligomers n-Py ($n = 6, 8, 15, 24$) with benzenoid structure. The colored line with squares in Fig. 1a depicts the same C—C bond lengths of the dication oligomer 6-Py^{2+}. The effect of bipolaron presence on the

Table 1
Binding energies of optimized oligopyrrole dication structures in singlet and triplet states at the B3PW91/6-31+G(d,p) level of theory. The grounds states are singlets for n-Py with $5 \leqslant n \leqslant 15$ and triplets otherwise. The last column, $E_{singlet}/n$, is an energy estimate of the pure singlet state [42]. Energies are in eV.

n-Py^{2+}	$E_{singlet}/n$	$E_{triplet}/n$	estimated $E_{singlet}/n$
5-Py^{2+}	−50.5096	−50.4489	−50.5096
6-Py^{2+}	−50.9199	−50.8987	−50.9199
7-Py^{2+}	−51.1919	−51.1825	−51.1919
8-Py^{2+}	−51.4037	−51.3960	−51.4097
9-Py^{2+}	−51.5481	−51.5437	−51.5518
10-Py^{2+}	−51.6577	−51.6553	−51.6600
11-Py^{2+}	−51.7432	−51.7418	−51.7444
12-Py^{2+}	−51.8118	−51.8109	−51.8126
15-Py^{2+}	−51.9524	−51.9523	−51.9525
18-Py^{2+}	−52.0384	−52.0385	−52.0383
21-Py^{2+}	−52.0961	−52.0963	−52.0958
24-Py^{2+}	−52.1372	−52.1375	−52.1369
27-Py^{2+}	−52.1678	−52.1681	−52.1675

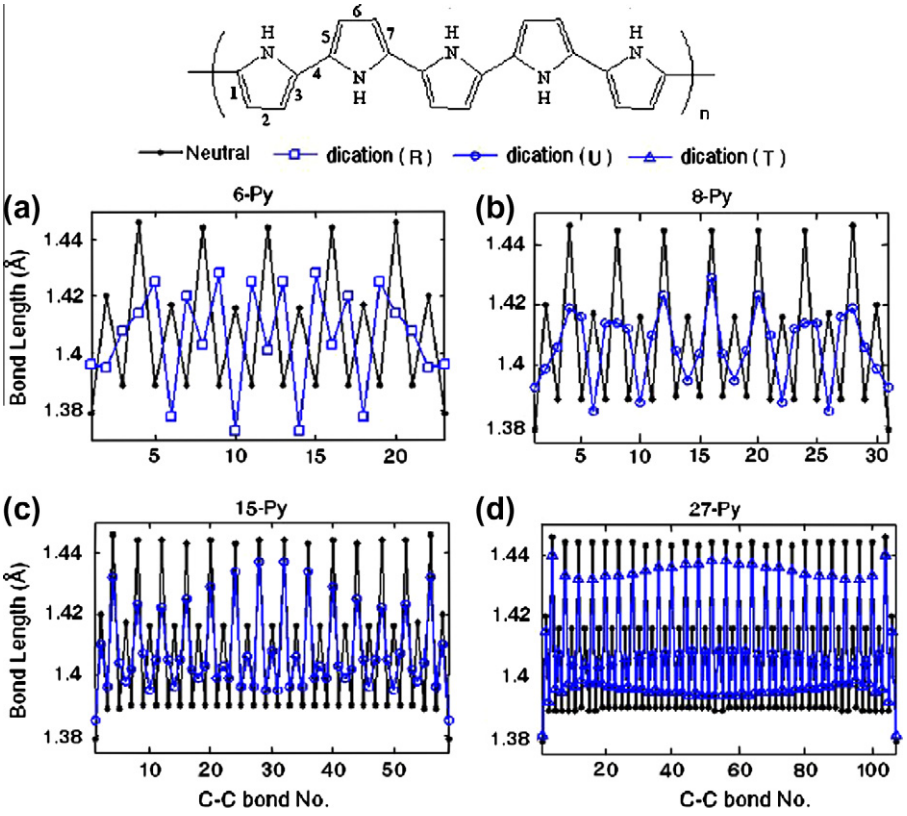

Fig. 1. C—C bond length along the conjugated chain for neutral and dication *n*-Py ($n = 6, 8, 15, 27$). Black lines depict the neutral oligomers and colored lines correspond to the dications. Restricted singlet calculation is R, unrestricted singlet calculation is U and T is triplet.

backbone C—C bond length alternation is clearly seen. The central part of the chain has acquired inter-monomer C—C bond lengths compatible with the quinoid phase of the oligomer. In fact the benzenoid phase has single C—C inter-monomer bonds of 1.44 Å. These bond lengths are depleted to 1.40 Å in the three central monomers, more consistent with the bond length of inter-monomer C—C double bonds characteristic of the quinoid phase. Meanwhile the colored line with circles in Fig. 1b–c shows the backbone C—C bond lengths when there is mixture between polaron pair and bipolaron. It is evident that the polaron pair produces a small and more homogeneous decrease in inter-monomer C—C bond lengths, impeding characterization of clear regions with quinoid structure. The most noticeable effect in medium-sized oligomer dications is the internal-to-monomer C—C bond length change, which is indicative of delocalization of the π electron cloud on each monomer ring. A similar effect, now extending along the full chain, is visible for the long oligomer dications as shown in Fig. 1d (colored line with triangles) where all internal-to monomer C—C bonds have basically the same bond length and the inter-monomer bonds are slightly shorter (1.435 Å) than in neutral oligomers. Delocalization of the π electrons over each monomer ring is evident.

Mulliken population analysis and NPA are used to analyze the charge distribution along the chain of oligomer dications. The total charge on each monomer as a function of its position along the chain is shown in Fig. 2. Figures on the left correspond to Mulliken population analysis, while figures on the right depict the charge distribution obtained within the NPA method. The top two plots of Fig. 2 illustrate results for the oligomer dication 6-Py^{2+} showing an appreciable charge localization on the two central monomers (third and fourth) characteristic of bipolaron formation. The central plots for 8-Py^{2+} and 15-Py^{2+} show the tendency of two polarons to split apart and localize toward the ends of the oligomer chain. The NPA results show this effect very clearly. Bottom plots illustrate the charge distribution when the ground state is a triplet, indicating that there is a fairly delocalized charge distribution along the length of the oligomer dication with a slightly larger charge localizing at the two oligomer ends.

A comparison between the electronic structure of neutral oligomers and their dications is provided in Fig. 3 showing changes in the HOMO–LUMO gap energy region. As expected, in the case of 6-Py^{2+}, the bipolaron is identified by the detachment of one state from the valence band and one state from the excited band. These states position themselves quite symmetrically within the HOMO–LOMO gap. This effect is also seen in 8-Py^{2+} and 15-Py^{2+}, although the two states are located asymmetrically in the gap. This asymmetry increases with the length of the oligomer as is characteristic of polaron-pairs. The case of 24-Py^{2+} shows clearly the formation of localized bands within the HOMO–LUMO gap, which enriches the optical spectrum.

The vibrational spectra and their IR-active intensities for 6-Py^{2+} and 12-Py^{2+} are depicted in Fig. 4. The IR active frequencies of both 6-Py^{2+} and 12-Py^{2+} singlet states (top in Fig. 4) are predominantly distributed in the region of 950–1700 cm^{-1}. The vibrational frequencies for the triplet state (bottom in Fig. 4) are distributed in the same spectral region. For 6-Py^{2+} the strongest vibrational frequency locates at 1629 cm^{-1} corresponding to N—H, C—H bending and C—C stretching motions. The second strong vibrational mode at 1433 cm^{-1} for the 6-Py^{2+} singlet state corresponds to a combination of N—H, C—H bending and N—C, C—C stretching motions, while the third high peak at 973 cm^{-1} is assigned to C—H bending and ring distortion motions. In the triplet state the former mode is slightly red shifted to 1429 cm^{-1}, while the second high peak at 1390 cm^{-1} also corresponds to a combination of N—H, C—H bending and C—C stretching motions. For 12-Py^{2+} the first four dominant vibrational modes for both states are located at 1615 cm^{-1} (N—H bending and C—C stretching), 1382 cm^{-1} (C—C stretching),

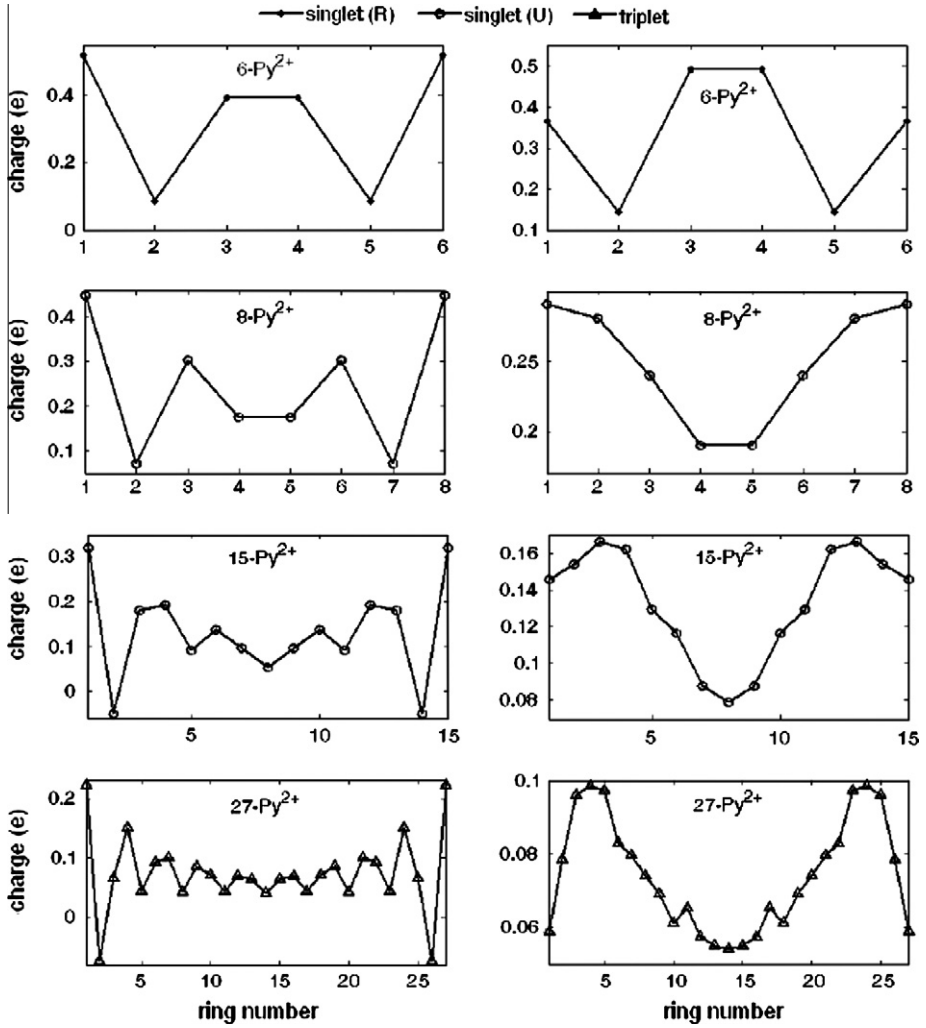

Fig. 2. Charge distribution along the chain of n-Py^{2+} ($n = 6, 8, 15, 27$). Mulliken population analysis results are on the left and NPA charges are on the right.

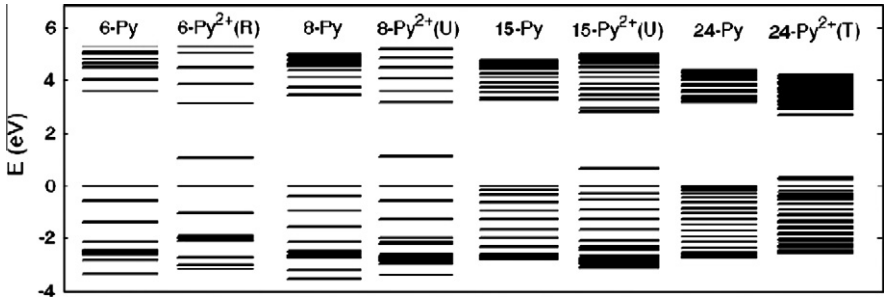

Fig. 3. Electronic structure of n-Py and n-Py^{2+} ($n = 6, 8, 15, 24$) showing the HOMO–LUMO energy gap. Restricted singlet calculation is R, unrestricted singlet calculation is U and T is triplet.

1501 cm^{-1} (C—C stretching and C—N stretching), and 1255 cm^{-1}) (N—H, C—H bending). This similarity proves that both states, singlet and triplet, of 12-Py^{2+} are not only close in energy but have similar curvature.

4. Conclusion

In summary, this hybrid DFT method study of n-Py dications shows that the short chain n-Py^{2+} ($n < 7$) oligomer dications display bipolarons, while in medium-sized oligopyrrole dications n-Py^{2+} ($6 \leqslant n \leqslant 16$) two polarons are formed in the ground singlet state. In long oligopyrrole dications, n-Py^{2+} ($n > 15$), the polaron pair becomes dominant but the ground state is a triplet. These observations are useful for the synthetic chemist indicating that the phase change benzenoid–quinoid occurring upon double-oxidation of the oligopyrroles will only occur in short regions of 3–4 monomers of polymer backbone. The only possibility to extend that spatial region is then to induce multiply charged oligomer cations [23]. Our observations are also useful to assert that when the

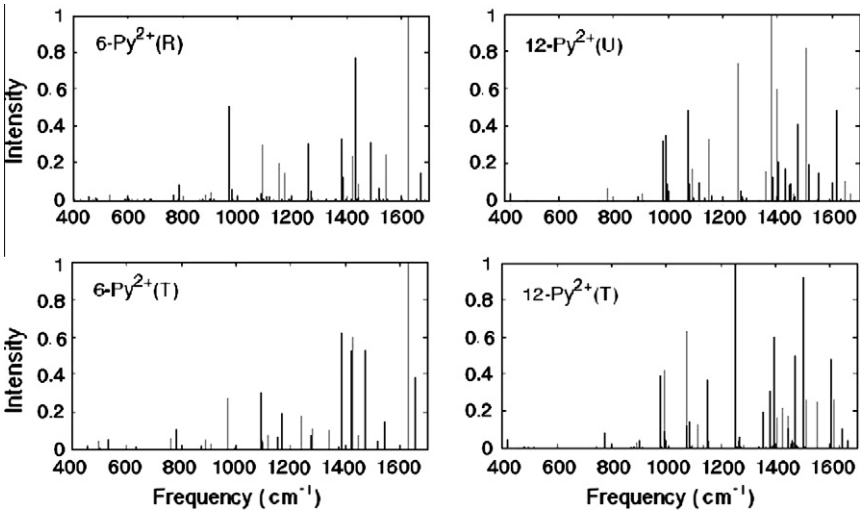

Fig. 4. Vibrational spectrum of the 6-Py^{2+} and 12-Py^{2+} in the singlet ground state (top) and triplet first excited state (bottom). Intensities are normalized to the highest peak in each spectrum.

phase of the polymer is quinoid, the charge carriers are bipolarons. Experimentally it has been observed that a high level of dopants 25–35% is needed to reach a full quinoid structure. Our results are in full agreement with this empirical fact.

Acknowledgements

We gratefully acknowledge support from NSFC, Project 11147184 supported by NSFC and from the Natural Science Foundation of the Jiangsu Higher Education Institutions of China (Grant No. 10KJB140003).

References

[1] A.R. Bishop, D.K. Campbell, K. Fesser, Polyacetylene and relativistic field theory models, Mol. Cryst. Liq. Cryst. 77 (1981) 253–264.
[2] S.A. Brazovskii, N.N. Kirova, Excitons, polarons and bipolarons in conducting polymers, JETP Lett. 33 (1981) 4–8.
[3] J.L. Bredas, R.R. Chance, R. Silbey, Comparative theoretical study of the doping of conjugated polymers: polarons in polyacetylene and polyparaphenylene, Phys. Rev. B: Condens. Matter 26 (1982) 5843–5854.
[4] W.P. Su, J.R. Schrieffer, Soliton dynamics in polyacetylene, Proc. Natl. Acad. Sci. USA 77 (1980) 5626–5629.
[5] G. Barbarella, L. Favaretto, G. Sotgiu, L. Antolini, G. Gigli, R. Cingolani, A. Bongini, Rigid-core oligothiophene-S,S-dioxides with high photoluminescence efficiencies both in solution and in the solid state, Chem. Mater. 13 (2001) 4112–4122.
[6] H. Hoppe, N.S. Sariciftci, Organic solar cells: an overview, J. Mater. Res. 19 (2004) 1924–1945.
[7] E. Smela, O. Inganas, I. Lundstrom, Conducting polymers as artificial muscles: challenges and possibilities, J. Micromech. Microeng. 3 (1993) 203–205.
[8] A.J.W. Tol, The instability of a bipolaron versus two polarons: charge localization in cyclo-dodecathiophene, Synth. Met. 74 (1995) 95–98;
A.J.W. Tol, The electronic and geometric structure of dications of oligothiophenes, Chem. Phys. 208 (1996) 73–79.
[9] G. Brocks, Polarons and bipolarons in oligothiophenes: a first principles study, Synth. Met. 102 (1999) 914–915.
[10] G.M.E. Silva, Electric-field effects on the competition between polarons and bipolarons in conjugated polymers, Phys. Rev. B 61 (2000) 10777–10781.
[11] S.S. Zade, M. Bendikov, Theoretical study of long oligothiophene dications: bipolaron vs polaron pair vs triplet state, J. Phys. Chem. B 110 (2006) 15839–15846.
[12] N. Zamoshchik, U. Salzner, M. Bendikov, Nature of charge carriers in long doped oligothiophenes: the effect of counterions, J. Phys. Chem. C 112 (2008) 8408–8418.
[13] Y. Furukawa, Electronic absorption and vibrational spectroscopies of conjugated conducting polymers, J. Phys. Chem. 100 (1996) 5644–15653.
[14] N. Colaneri, M. Nowak, D. Spiegel, S. Hotta, A. Heeger, Bipolarons in poly(3-methylthiophene): spectroscopic, magnetic, and electrochemical measurements, Phys. Rev. B 36 (1987) 7964–7968.
[15] D. Fichou, G. Horowitz, B. Xu, F. Gamier, Stoichiometric control of the successive generation of the radical cation and dication of extended α-conjugated oligothiophenes: a quantitative model for doped polythiophene, Synth. Met. 39 (1990) 243–259.
[16] J.A.E.H. van Haare, E.E. Havinga, J.L.J. van Dongen, R.A.J. Janssen, J. Cornil, J.L. Bredas, Redox states of long oligothiophenes: two polarons on a single chain, Chem. Eur. J. 4 (1998) 1509–1522.
[17] J.J. Apperloo, R.A.J. Janssen, P.R.L. Malenfant, L. Groenendaal, J.M.J. Frechet, Redox states of well-defined π-conjugated oligothiophenes functionalized with poly(benzyl ether) dendrons, J. Am. Chem. Soc. 122 (2000) 7042–7051.
[18] A.J. Heeger, S. Kivelson, J.R. Schrieffer, W.P. Su, Solitons in conducting polymers, Rev. Mod. Phys. 60 (1988) 781–850.
[19] J.L. Bredas, G.B. Street, Polarons, bipolarons, and solitons in conducting polymers, Acc. Chem. Res. 18 (1985) 309–315.
[20] Y. Shimoi, M. Kuwabara, S. Abe, Highly doped nondegenerate conjugated polymers-a theory using the DMRG method, Syn. Met. 119 (2001) 213–214.
[21] M.J.L. Santos, A.G. Brolo, E.M. Girotto, Study of polaron and bipolaron states in polypyrrole by in situ Raman spectroelectrochemistry, Electrochim. Acta 52 (2007) 6141–6145.
[22] R. Colle, A. Curioni, Density-functional theory study of electronic and structural properties of doped polypyrroles, J. Am. Chem. Soc. 120 (1998) 4832–4839.
[23] Y. Dai, E. Blaisten-Barojas, Energetics, structure, and charge distribution of reduced and oxidized n-pyrrole oligomers: a density functional approach, J. Chem. Phys. 129 (2008) 164903.
[24] Y. Dai, E. Blaisten-Barojas, Monte Carlo study of oligopyrroles in condensed phases, J. Chem. Phys. 133 (2010) 034905.
[25] Y. Dai, S. Chowdhury, E. Blaisten-Barojas, Density functional theory study of the structure and energetics of negatively charged oligopyrroles, Int. J. Quant. Chem. 111 (2011) 2295–2305.
[26] J.M. Andre, D.P. Vercauteren, G.B. Street, J.L. Breda, Electronic properties of polypyrrole: an ab initio Hartree Fock study, J. Chem. Phys. 80 (1984) 5643–5648.
[27] X. Lin, E. Smela, S. Yip, Polaron-induced conformation change in single polypyrrole chain: an intrinsic actuation mechanism, Int. J. Quant. Chem. 102 (2005) 980–985.
[28] A.D. Becke, Density-functional thermochemistry. III. The role of exact exchange, J. Chem. Phys. 98 (1993) 5648–5652.
[29] J.P. Perdew, J.A. Chevary, S.H. Vosko, K.A. Jackson, M.R. Pederson, D.J. Singh, C. Fiolhais, Atoms, molecules, solids, and surfaces: applications of the generalized gradient approximation for exchange and correlation, Phys. Rev. B 46 (1992) 6671–6687.
[30] J.P. Perdew, K. Burke, Y. Wang, Generalized gradient approximation for the exchange-correlation hole of a many-electron system, Phys. Rev. B 54 (1996) 16533–16539.
[31] R. Krishnan, J.S. Binkley, R. Seeger, J.A. Pople, Self-consistent orbital methods. XX. A basis set for correlated wave functions, J. Chem. Phys. 72 (1980) 650–654.
[32] M.J. Frisch, G.W. Trucks, H.B. Schlegel, G.E. Scuseria, M.A. Robb, J.R. Cheeseman, J.A. Montgomery Jr., T. Vreven, K.N. Kudin, J.C. Burant, J.M. Millam, S.S. Iyengar, J. Tomasi, V. Barone, B. Mennucci, M. Cossi, G. Scalmani, N. Rega, G.A. Petersson, H. Nakatsuji, M. Hada, M. Ehara, K. Toyota, R. Fukuda, J. Hasegawa, M. Ishida, T. Nakajima, Y. Honda, O. Kitao, H. Nakai, M. Klene, X. Li, J.E. Knox, H.P. Hratchian, J.B. Cross, V. Bakken, C. Adamo, J. Jaramillo, R. Gomperts, R.E. Stratmann, O. Yazyev, A.J. Austin, R. Cammi, C. Pomelli, J.W. Ochterski, P.Y. Ayala, K. Morokuma, G.A. Voth, P. Salvador, J.J. Dannenberg, V.G. Zakrzewski, S. Dapprich, A.D. Daniels, M.C. Strain, O. Farkas, D.K. Malick, A.D. Rabuck, K. Raghavachari, J.B. Foresman, J.V. Ortiz, Q. Cui, A.G. Baboul, S. Clifford, J.

Cioslowski, B.B. Stefanov, G. Liu, A. Liashenko, P. Piskorz, I. Komaromi, R.L. Martin, D.J. Fox, T. Keith, M.A. Al-Laham, C.Y. Peng, A. Nanayakkara, M. Challacombe, P.M.W. Gill, B. Johnson, W. Chen, M.W. Wong, C. Gonzalez, J.A. Pople, Gaussian 03, Revision C.01, Gaussian, Inc., Wallingford, CT, 2004.

[33] C. Lee, W. Yang, R.G. Parr, Development of the Colle–Salvetti correlation-energy formula into a functional of the electron density, Phys. Rev. B 37 (1988) 785–789.

[34] P.J. Stephens, F.J. Devlin, C.F. Chabalowski, M.J. Frisch, Ab initio calculation of vibrational absorption and circular dichroism spectra using density functional force fields, J. Phys. Chem. 98 (1994) 11623–11627.

[35] A.D. Boese, J.M.L. Martin, Development of density functionals for thermochemical kinetics, J. Chem. Phys. 121 (2004) 3405–3416.

[36] J.P. Perdew, K. Burke, M. Ernzerhof, Generalized gradient approximation made simple, Phys. Rev. Lett. 77 (1996) 3865–3868;
J.P. Perdew, K. Burke, M. Ernzerhof, Generalized gradient approximation made simple, Phys. Rev. Lett. 78 (1997) 1396.

[37] Y. Zhao, D.G. Truhlar, Density functional for spectroscopy: no long-range self-interaction error, good performance for Rydberg and charge-transfer states, and better performance on average than B3LYP for ground states, J. Phys. Chem. A 110 (2006) 13126–13130.

[38] L. Nygaard, J.T. Nielsen, J. Kirchheiner, G. Maltesen, J. Rastrup-Andersen, G.O. Sorensen, Microwave spectra of isotopic pyrroles: molecular structure, dipole moment, and N quadrupole coupling constants of pyrrole, J. Mol. Struct. 3 (1969) 491–506.

[39] A.E. Reed, F. Weinhold, Natural bond orbital analysis of near-Hartree-Fock water dimer, J. Chem. Phys. 78 (1983) 4066–4073.

[40] C. Peng, P.Y. Ayala, H.B. Schlegel, M.J. Frisch, Using redundant internal coordinates to optimize equilibrium geometries and transition states, J. Comp. Chem. 17 (1996) 49–56.

[41] Y. Gao, C.G. Liu, Y.S. Jiang, Electronic structure of thiophene oligomer dications: an alternative interpretation from the spin-unrestricted DFT study, J. Phys. Chem. A 106 (2002) 5380–5384.

[42] K. Yamaguchi, F. Jensen, A. Dorigo, K.N. Houk, A spin correction procedure for unrestricted Hartree-Fock and Moller-Plesset wavefunctions for singlet diradicals and polyradicals, Chem. Phys. Lett. 149 (1988) 537–542.